

Effect of joint stiffness on standing stability

W. Thomas Edwards*

*Department of Rehabilitation Engineering, Rehabilitation Engineering Analysis Laboratory,
Kessler Medical Rehabilitation Research and Education Corporation, 1199 Pleasant Valley Way,
West Orange, NJ 07052, United States*

Received 15 September 2005; received in revised form 9 May 2006; accepted 14 May 2006

Abstract

Standing balance depends on the effective control of the torques at the ankle, knee, and hip. Stiffness at each joint and feedback proportional to joint angle contributes to these torques and to postural stability. This study examines the interaction of multiple joints on the minimum effective joint stiffnesses needed to maintain quiet standing and determines the inherent patterns of sway motion based on dynamic calculations of a four-link, three-joint, sagittal plane model. The equations of motion for quiet standing are solved to obtain the limits of stability for an individual (75 kg, 1.753 m tall) considering different combinations of joint stiffness. These calculations demonstrate that the single-link inverted pendulum model provides a less conservative estimate of minimum stiffness. That is, more stiffness is required at each joint to preserve stability when rotation is permitted at the knee and hip joints. Based on these analyses, the well recognized ankle and hip balance strategies appear to correspond to variations of the inherent patterns of motion of the lowest frequency mode. Additional calculations show that the stability decreases with an increase in body mass index. The present results quantify the interaction of the combined active and passive stiffnesses at the ankle, knee, and hip, and identify the minimum conditions needed for quiet standing. These criteria define standing-balance stability thresholds needed to assess the risk of falling and to guide rehabilitation.

© 2007 Elsevier B.V. All rights reserved.

Keywords: Biomechanics; Joint stiffness; Postural control; Balance; Stability threshold

1. Introduction

The contribution of the effective joint stiffness to stability during standing has been questioned in several previous studies. Winter et al. proposed that joint stiffness alone may be sufficient to control stability and that a minimum ankle joint stiffness defines a threshold for stability [1]. They interpreted the dynamics of standing based on a simple inverted pendulum model of the body with effective joint stiffness providing a restoring torque at the ankle. They estimated that a combined ankle stiffness of 850 N m/rad is sufficiently large to provide stability for a 70 kg individual [1,2]. The effective joint stiffness described was the change in torque for a change in rotation resulting from all passive and active contributions. These active and passive components of stiffness depend on the level of muscle contraction

in addition to the joint angle and angular velocity [3–5] and are mechanically indistinguishable [6], unless the reflex component is experimentally blocked [7].

Morasso and Schieppati re-examined the Winter et al. findings and found two shortcomings in the stiffness balance model [8]. First, they demonstrated the importance of the underlying dynamic processes and showed that in quiet stance the center of pressure and the center of mass move in-phase as a consequence of physics. This response is independent of a control strategy. Second, they argued that the physiological ankle stiffness can be only about 400 N m/rad, based on earlier studies [9] and that this stiffness is not adequate to stabilize body sway. However, these studies considered only the ankle in a single-link inverted pendulum representation and did not consider the effects of hip and knee rotations on postural control [1,2,8,10].

The combined effects of the ankle, knee and hip can be examined by extending the single link inverted pendulum to a dynamic multi-segment model. The required equations of

* Tel.: +1 973 324 3539; fax: +1 973 243 6984.

E-mail address: tedwards@kmrrec.org.

Nomenclature

The symbols used in the equations define the properties of the model segments for a 75.3 kg individual, 1.753 m tall. The subscripts are:

s = shank; t = thigh; b = body; a = ankle; k = knee; h = hip.

Symbol	Description	Values
m_s, m_t, m_b	Segment masses excluding feet. Total of left plus right (kg)	6.478, 15.059, 51.6481
I_s, I_t, I_b	Moment of inertia of each segment about its center of mass (kg m^2)	0.122, 0.291, 3.012
h_s, h_t	Length of the shank and thigh model segments (m)	0.431, 0.430
e_s, e_t, e_b	Distance from the distal end of each segment to its center of mass (m)	0.245, 0.244, 0.356
$\theta_a, \theta_k, \theta_h$	Joint rotations at the ankle, knee and hip (positive as shown in Fig. 1)	variables
g	Gravity constant (m/s^2)	9.8
\mathbf{q}	The generalized coordinates, $\mathbf{q} = [\theta_a \ \theta_k \ \theta_h]^T$	variables
$\mathbf{A}, \mathbf{B}, \mathbf{C}$	Coefficient matrices (3×3) for the moments due to angular accelerations (\mathbf{A}), the angular velocities (\mathbf{B}), and rotations (\mathbf{A}). These coefficients were collected from the linearized equations of motion	Eq. (A.3)
a_{ij}, b_{ij}, c_{ij}	The coefficients of the $\mathbf{A}, \mathbf{B}, \mathbf{C}$ (3×3) matrices. The subscripts correspond to the rotations of the three joints, ordered $i = 1, 2, 3$ for ankle, knee, and hip	Eq. (A.3)
K_a, K_k, K_h	Effective stiffness at the joints due to passive tissues and to muscle contractions that are proportional to the change in the joint angle	Values varied

motion have been derived for analogous multi-link, multi-joint systems of the upper extremity, lower extremity and standing. Simple dynamic studies of the shoulder and arm have been presented that were based on the analysis of a two-link model of the upper arm and forearm/hand with a stationary shoulder [11]. A seven-link model (head, trunk, two upper and three lower extremity links) was used to study

the planar kinetics of somersaults on a trampoline [12]. The analyses of the swaying motions during standing were presented for more detailed multi-link descriptions [13,14]. Four-segment models of sagittal standing include an independent upper body, thigh, lower leg, and stationary feet links [15,16]. The results from the multi-joint models in each case demonstrate significant interactions between the segments. The response at one joint is dependent on the properties of adjacent segments and the rotations at other joints.

The equations of motion of these multi-segment models describe the inherent behavior of the system (described by segment mass, damping and stiffness parameters) and the interaction of the system with the external loads. The natural response reflects both the inherent patterns of motion and the stability of the dynamic system. The number of distinct patterns of motion (modes) and the number of natural frequencies (characteristic frequencies) are equal to the number of independent modeled motions, the degrees of freedom of the system. Therefore, a single-link model requires one equation to describe segment motion around a single moving joint with the other joints rigid, for example bending about the ankle or the hip. One equation is added to the model for each additional independent motion. In the case of a four-link, three-joint (ankle, knee, and hip) model of standing, there are three equations that describe three characteristic frequencies and three modes.

In the present study, a model of quiet standing (defined by the equations of motion) was developed considering the relative motions across the ankle, knee, and hip joints. The goal was to determine how rotations at the knee and hip influence stability in comparison to the single-link inverted pendulum with only ankle rotation. The main objectives were to calculate the limits of stability for a range of lower extremity joint stiffnesses and to determine the effect of different values of body mass on the stability limits.

2. Method

2.1. Equations of motion for standing based on joint angles

The dynamic equations of motion for a three-joint, four-link sagittal model of standing were derived using Lagrange's Method. The properties of the left and right legs were combined to provide the sagittal, flexion–extension stiffnesses at the ankle, knee, and hip, and combined mass properties for the shank and thigh. The mass of the body was modeled in four segments representing the upper body, thighs, lower leg, and feet. The upper body segment included the arms, head, neck and trunk. Each leg segment combined the properties for left and right sides (Fig. 1). Using the model, the limits of stability were identified for a range of values of body mass, body height, and the joint stiffnesses.

The nonlinear equations of motion were derived and then checked using MathCad (Version 11.1, Mathsoft Engineering & Education, Inc.) and Mathematica (version 5, Wolfram Research, Inc.). A vector of the generalized coordinates, $\mathbf{q} = [\theta_a \ \theta_k \ \theta_h]^T$, was used to describe the sagittal rotations between adjacent segments at the ankle (θ_a), knee (θ_k), and hip (θ_h) (Fig. 1). An independent rotation of each segment was permitted with the exception of the feet, which were fixed at the floor. These nonlinear equations of motion are detailed in the Appendix.

The nonlinear equations of motion were linearized about the neutral upright position. In quiet standing, each of the joint angles and angular velocities is small, so that $\cos(a) \approx 1$ and $\sin(a) \approx a$. For small rotations in quiet standing, the equations of motion simplify:

$$\mathbf{A}\ddot{\mathbf{q}} + \mathbf{B}\dot{\mathbf{q}} + \mathbf{C}\mathbf{q} = \mathbf{T} \quad (1)$$

The linearized inertia matrix (\mathbf{A}) and the stiffness matrix (\mathbf{C}) are constant and symmetric. The stiffness matrix \mathbf{C} is the 3×3 matrix of the partial derivatives of the potential energy of the system with respect to the three joint rotations. The coefficients for these matrices are shown in the Appendix. The joint stiffnesses provide torques that are proportional to joint rotation. These result from the passive stiffness and from the torque produced by muscle contraction that is proportional to changes in the joint angle. In keeping with earlier analyses, no interaction was included between the joint stiffnesses and no damping, a torque proportional to rotational velocity, was included, $\mathbf{B} = 0$. The active and externally applied joint torques (\mathbf{T}) are not proportional to either joint angle or the joint angular velocity. These external torques shown in the equation do not contribute to the calculations of the eigenvalues and eigenvectors of the equations of motion.

The natural modes of response and the natural frequencies, described by the eigenvectors and eigenvalues of the equations of motion of this dynamic system, were calculated from Eq. (1). There are three distinct eigenvectors, patterns of motion, for the standing model with rotations at the ankle knee and hip.

2.2. Segment and joint properties—limits of stability

The stability boundaries for the least stable mode were calculated over a range of conditions. The joint stiffnesses of the ankle and hip were varied from 0 to 2000 N m/rad. The stiffness of the knee was varied from 600 N m/rad up to completely rigid. The values represent the combined stiffness of both legs.

Values for coefficients of the \mathbf{A} and \mathbf{C} matrices were calculated for standing equilibrium using the geometry and mass of the 50th percentile male from a study of U.S. HEW civilians, tabulated by Chaffin and Anderson [17]. These values correspond to an individual, height = 1.753 m and body weight = 75.2 kg, with center of mass 1.02 m above the ankle and a combined mass of 73.18 kg in the body

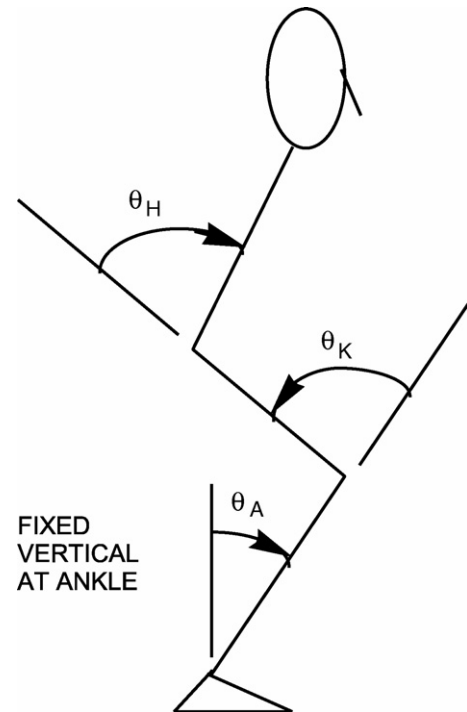


Fig. 1. Representation of the joint angles of the ankle, knee, and hip. The joint angle convention shown in the figure was used in the model and equations presented.

segments above the ankle. The inertia about the center of mass was 11.11 kg m^2 , or equivalent to an inertia of 87.10 kg m^2 with respect to the ankle. The segment geometry, mass, and inertia properties are listed in the Appendix for this nominal configuration.

If the joint stiffnesses are reduced, the natural frequencies decrease and finally become unstable when the frequency of the eigenvalue representing the lowest sway frequency reach 0. This can be visualized by considering a root-locus diagram of the eigenvalues near this condition (Fig. 2). The individual points defining the stability threshold contours were defined by plotting multiple root-locus diagrams as the joint stiffnesses were varied. For each root-locus plot, the crossing of the lowest frequency mode through 0 and into the right half-plane, indicated the loss of stability and a divergence from the upright position, a fall.

2.3. Effect of body mass and height

The effects of body mass and height on standing stability also were considered. The variation in frequency of the least stable mode was calculated for a range of values of body mass index from 18 to 30 kg/m^2 . Curves for the stability limit were calculated for three body heights (1.611, 1.753, and 1.895 m) corresponding to the mean height used in the model $\pm 1 \text{ S.D.}$ [17]. As the body mass index was varied, the joint stiffnesses were held constant at $K_a = 1170 \text{ N m/rad}$, $K_k = 1200 \text{ N m/rad}$ and $K_h = 700 \text{ N m/rad}$.

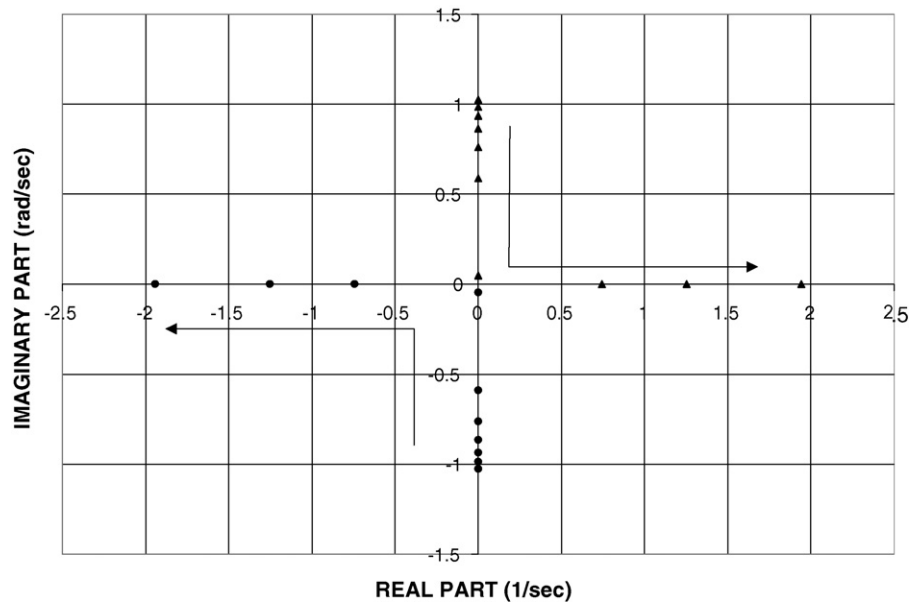


Fig. 2. A root-locus plot used to identify a single threshold point. The real and imaginary components of the least stable mode were plotted as a function of the hip stiffness. The complex conjugate root pair was calculated at increments of 100 N m/rad as K_h decreased from 1000 to 100 N m/rad. For this plot ankle and knee stiffness were constant, $K_a = 1118$ N m/rad and $K_k = 2000$ N m/rad. The system becomes unstable when one of the two roots (the triangle symbol) becomes a positive-real number, as K_h decreases to just below 400 N m/rad. The stability limit condition occurs when a root reaches a frequency of 0.

3. Results

The stability limits for combinations of the effective joint stiffnesses of ankle, knee, and hip are shown in the contour plot (Fig. 3). The curves in the figure are bounded by two limiting cases, one with rotation only at the ankle and the other with rotation only at the hip. These two conditions are the asymptote lines in the figure bounding the other multi-joint stability contours. The model for ankle rotation only, with rigid knee and hip joints, is unstable for all values of ankle stiffness (K_a) less than 731.3 N m/rad and the model with hip rotation only becomes unstable for values of hip stiffness (K_h) less than 179.7 N m/rad. For other combinations of ankle, knee, and hip stiffnesses, all joint stiffness combinations below and to the left of the 'RIGID' knee contour line are unstable. Considering individual contour points, the results show, if the stiffness of one of the three joints is reduced with respect to a set of threshold stiffness values, balance becomes unstable. On the other hand, if a joint stiffness is higher than the stability threshold value, stability improves. The results indicate that as the stiffness of one joint decreases, larger values of stiffness at the other two joints are needed.

The characteristic patterns of motion were obtained from the eigenvectors of Eq. (1). The relative magnitudes of joint rotations from the eigenvector of the lowest frequency, least stable mode were compared. For those conditions along the diagonal, dashed-line in Fig. 3, the ankle and hip rotations are equal. Above this line the hip rotation is less than the ankle rotation; below this line the ankle rotation is less than the hip rotation for this least stable mode. The sway oscillations of this least stable mode display rotations in the

same direction at the ankle and hip. The next higher mode at 1.50 Hz, the ankle and hip rotations are in the opposite directions as shown in Fig. 4.

The variation in the frequency of the least stable mode (pattern of motion) for a range of body mass index is shown

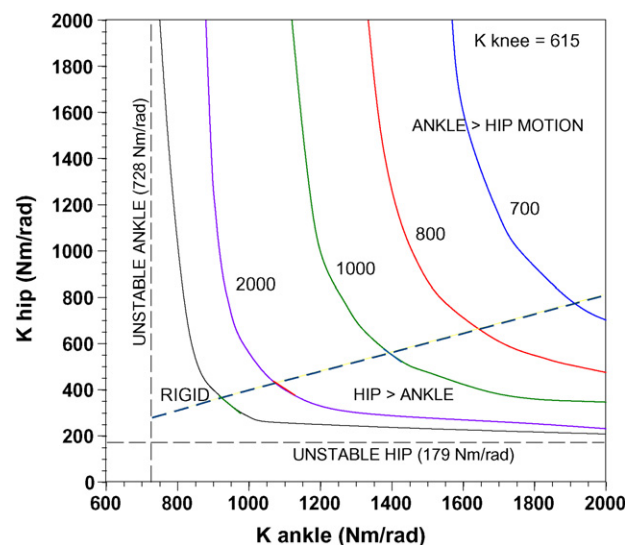


Fig. 3. Stability limits for combinations of ankle, knee, and hip stiffnesses. The contour curves of neutral stability (for a mean sized male 1.753 m tall, weighing 75.2 kg) are plotted for fixed values of knee stiffness. Four contour curves are shown for $K_k = 700, 800, 1000, 2000$, and Rigid as the ankle and hip stiffnesses vary. The knee stiffness $K_k = 600$ N m/rad at upper right corner of the plot, $K_a = K_h = 2000$ N m/rad. Each point on or above the 'Rigid' contour corresponds to a combination of minimum ankle, knee and hip stiffnesses sufficient for stable standing. Combinations of stiffnesses above the diagonal, dashed line have larger ankle motion than hip motion and combinations below have larger hip rotations than ankle rotations.

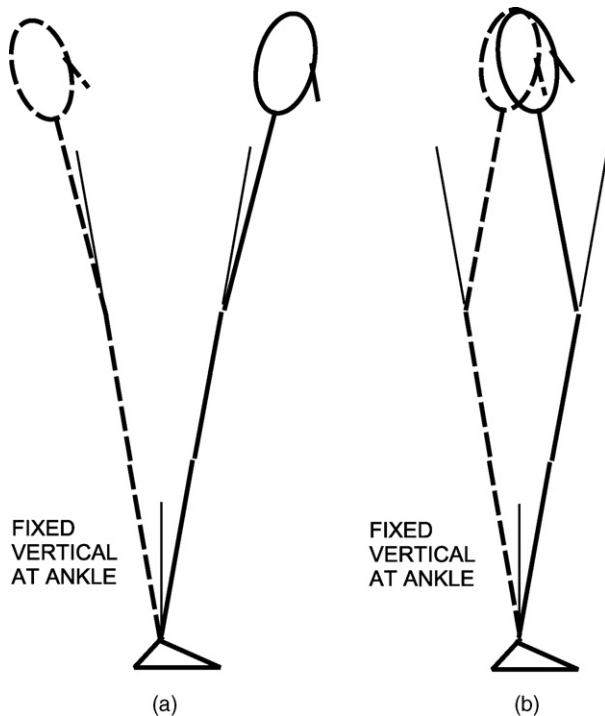


Fig. 4. (a and b) Patterns of motion of the least stable modes. The patterns of motion for the first two modes, obtained from the corresponding normalized eigenvectors assuming that the knee is locked ($K_k = 2000$ N m/rad) and the stiffnesses at the ankle and hip are $K_a = 950$ N m/rad and $K_h = 738$ N m/rad. The ratio of hip to ankle rotation of the lowest frequency mode (frequency = 0.002 Hz) is 0.43 with sway rotation in the same direction. (a) The ratio of hip to ankle rotation was -2.07 for the second (frequency = 1.50 Hz) mode. (b) The solid and dashed lines indicate the extreme displacements of one cycle of motion with ankle rotation scaled to 10° in both figures. The actual magnitudes of joint rotations generally will be less and depend on the initial conditions and external disturbances.

in Fig. 5. The joint stiffnesses were held constant at 1170, 1200 and 700 N m/rad at the ankle, knee, and hip, respectively. The three curves from upper to lower correspond to three body heights, 1.611, 1.753 and 1.895 m, respectively. Along each curve, there is a decrease in stability with increasing body mass index, a larger body mass with respect to body height.

4. Discussion

This study addresses aspects of theoretical questions raised by the prior investigations and the interpretation of the postural control response. The objective of the study was to calculate the limits of postural stability with respect to the stiffness of the ankle, knee and hip and to determine the effect of body mass on the stability limits. These results were compared to the findings of earlier studies that considered a single-link, inverted pendulum model.

4.1. Dynamic equations of motion

Postural control of spontaneous sway has been studied using both dynamic mechanical and control-based models. Although these modeling approaches are different in form, both describe the generation of corrective torque at the joints of the lower extremity needed to resist gravity. Mechanical models, such as those considered by Winter et al. [1,2], Johansson et al. [18] and others, incorporate spring stiffness and damping to represent ankle torques that are proportional to angle and angular velocity. In the control-based models, the equivalent stiffness and damping are modeled through

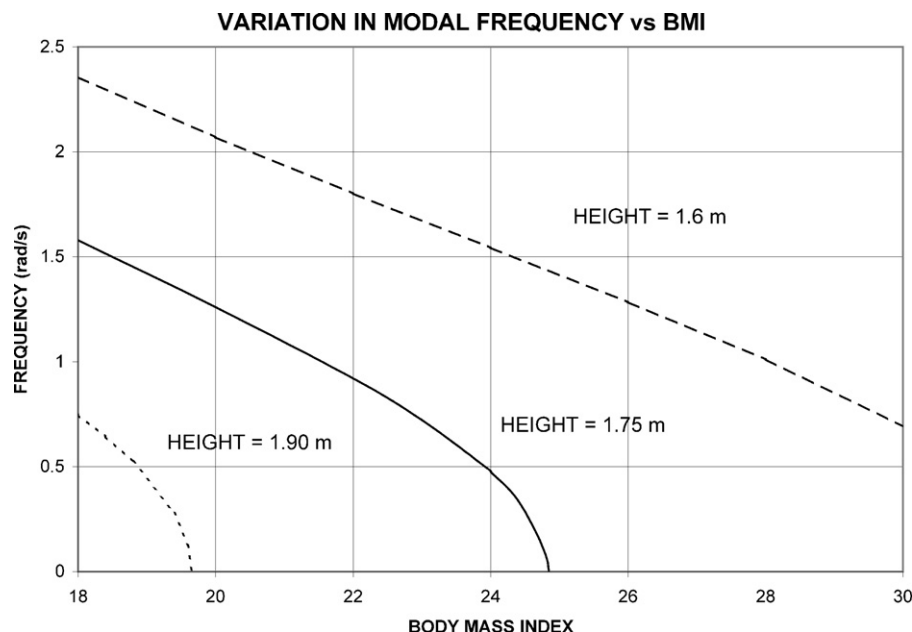


Fig. 5. Variation of modal frequency with body mass index. A plot of the eigenvalue, frequency (rad/s), of the least stable mode as body mass index is varied. The curves correspond to the results for three body heights (1.611, 1.753, and 1.895 m). Zero frequency corresponds to the threshold of stability.

the use of gains to produce joint torque. Feedback from the sensory systems can be included using proportional-derivative [19,20] or proportional-integrating-derivative controllers [18]. Neuro-mechanical and feedback delays may also be included in these control models [19–21]. A limitation of the application of either modeling approach is that those studies have been limited to a single degree of freedom reflecting only ankle rotations. Therefore, these models are unable to assess the interaction of hip and knee rotations.

The present study first addressed the questions, whether joint stiffness can stabilize balance and to what degree does the flexibility at three levels (the ankle, knee, and the hip) alter stability. There were several difficulties in resolving these questions. The first is the use of different definitions of stiffness in previous studies. The effective stiffness has been incorporated in balance models using a control gain proportional to joint angle (for example, see Masani et al. [19]). Peterka refers to a corrective torque that occurs without time delay as a passive torque and the remaining torque provided by muscle activation as active torque [20]. Others use the terms intrinsic mechanical stiffness to refer to the passive component and neural stiffness to refer to the active component of stiffness [22,23]. The underlying problem in either case is to identify the portion of joint torque, due to feedback, that is proportional to joint angle. This active torque can be represented as a contribution to joint stiffness and is not easily distinguishable from passive joint stiffness. This was interpreted further by Morasso and Sanguineti who observed that the effective or total ankle stiffness is a combination of three contributing systems: the passive elasticity at the ankle, the torque due to segmental reflexes, and the anticipatory or voluntary torque generated by descending motor commands [5].

A second difficulty in determining whether balance can be achieved by the control of the effective or total joint stiffness, is the assumption that stiffness of sufficient magnitude can be produced. A limited number of ankle and knee stiffness measurements have been presented. Weiss et al. tracked changes in dynamic stiffness of the human ankle joint over a wide range of muscle contraction levels, from rest to maximum voluntary contractions with subjects reclining supine on an experimental table [24]. Hof reported the series elastic stiffness of the ankle plantar-flexors, the triceps surae group, the combined soleus, medial and lateral gastrocnemius [9]. That study measured stiffnesses between 250 and 400 N m/rad (mean = 306 ± 39 N m/rad) for one leg at an ankle torque of 100 N m. The passive torque provided by the antagonists appears to contribute an additional 25 N m/rad for each leg. Lark et al. measured ankle stiffness between 229 and 498 N m/rad during stepping down for one leg in the older and the strongest young male subjects, respectively [25]. Loram and Lakie measured ankle stiffness for small perturbations while balancing an inverted pendulum or while standing free and compared results to an estimated critical stiffness, $K_{\text{criti-}}$

$\text{cal} = mgh$, where m is the mass of the body, g the gravity, and h is the height of the body center of mass over the ankle. They found that ankle stiffness for different subjects ranged from 0.36 to 1.35 times the critical value with a mean of 0.91 ± 0.23 (297.9 ± 68.8 N m/rad) [23]. Casadio et al. used a larger $1^\circ/150$ ms perturbation to measure the intrinsic ankle stiffness and found ankle stiffness to be $64 \pm 8\%$ of the critical stiffness [22]. The stiffness of the knee during maximum voluntary contraction of healthy subjects was measured. McHugh and Hogan found for one leg, that the highest stiffness (441 N m/rad) occurred at 70° of flexion [26]. From these studies, it appears that joint stiffness is low, but can approach the critical value of stiffness needed to provide stability for the single link inverted pendulum [5,8]. However, joint stiffnesses are less adequate considering flexibility at the ankle, knee, and hip. Additional joint stiffness data is needed during standing.

4.2. Study limitations

This is a theoretical study that focuses on observations drawn from the single-link, single-joint and the four-link, three-joint sagittal inverted pendulum models. Although models could be conceived that are more comprehensive, the present approach was chosen as an incremental extension of the inverted pendulum. The joint torques are produced by active and passive contributions. As modeled here and in the prior studies discussed above, the use of stiffness implies the instantaneous proportional response of the system to changes in the joint angles. The level of muscle activation and co-contraction is implicitly incorporated in the stiffness coefficients. There appears to be little consensus on the magnitudes of the joint stiffnesses, so a range of values were examined for each joint.

An additional assumption was that there were no interactions of the stiffnesses due to muscles that span two joints, such as the rectus femoris and the gastrocnemius muscles. These muscles interact mechanically with the rotations at both the hip and knee or the knee and ankle. Through these muscles, the rotation at one joint can produce a torque at the second joint, resulting in a stiffness coupling. Clearly, a more definitive description of ankle, knee and hip stiffness associated with different conditions and activities is needed.

The analyses also did not include velocity dependent torque or time delays found in sensory feedback systems. The contribution of damping associated with the velocity of joint rotation has been examined through experiments and simulations of quiet standing. Masani et al. studied the effect of combinations of gains proportional to joint angle and velocity on postural control [19]. They arbitrarily chose for their model a gain proportional to displacement of 20 N m/deg (1146 N m/rad) and either low or high derivative gain factors. They found for these gain values that both conditions were stable by Nyquist analysis. The study also included time delays. They noted that a pure proportional controller

with neuro-mechanical and feed back delays applied to the inverted pendulum was unstable. As shown in the contour plot of the stability thresholds (Fig. 3) the value chosen for the proportional gain factor is well above the ankle stiffness required for stability of the single link model. While damping or torques that are proportional to the angular velocity of the joints should tend to improve standing stability, delays will reduce the stability. So the loss of stability described by Masani et al. must be attributed to the delays applied to the system.

4.3. Stability contours and patterns of motion

A parametric approach was used to provide an estimate of the stability thresholds for joint stiffness combinations. Considering the potential range of joint stiffnesses possible at the ankle, knee, and hip, these results extend past investigations and provide the limits of stability and the representative patterns of motion for varying body mass, height, and joint stiffnesses. For conditions in which there is flexibility at all three joints, there are interactions between the rotations at the joints that tend to reduce stability in comparison to these two rigid cases (Fig. 3). With flexibility at both the ankle and hip, the stiffness required for stability is greater than the critical value indicated previously [5,8,22,23].

The patterns of motion calculated along the stability contours also suggest that alternative strategies, not reflected by the simple inverted pendulum model, contribute to the maintenance of balance. Earlier observations provide a basis for the so-called ankle and hip balance strategies and demonstrate that both the ankle and the hip should be included in postural stability models [27–29]. Appropriate combinations of ankle, knee, and hip stiffness can provide stable conditions with patterns of motion in which either hip rotation is greater than ankle rotation or those with ankle rotation greater than hip rotation. Although emphasis is generally placed on the use of an ankle strategy for balance, there is evidence indicating that control of hip rotation can be essential for those with balance deficits. The rotation at the hip can be greater and occur at higher velocities than rotation at the ankle [30]. When motion is restricted at the hip by using a stiff splint in healthy young individuals, ankle sway increases [31]. Kuo and Zajac found that rotation about the ankles only, requires more muscle activation than the “hip strategy” for a given amount of horizontal acceleration [28]. They proposed that the use of hip motions rather than ankle motions may be more effective and efficient for maintaining balance for some individuals [28]. Such studies demonstrate that control at the hip contributes to stable posture.

4.4. Effect of body mass

The results concerning the second objective of this study, to determine the effect of different values of body mass on the stability limits, were unexpected. Others have shown that an increased body mass index tends to reduce the risk of

hip fractures due to a reduced risk of falling [32]. The calculations here, of the limits of stability for a range of body mass index body mass index from 18 to 30 kg/m², show that there is a decrease in overall stability as the body mass index, increases. This finding suggests that factors, other than mass alone, must correlate with increased body mass index to improve stability and fracture risk. Although few longitudinal studies have been conducted, Taggart et al. found in their study of 287 elderly a significant change in bone mineral density with weight [33]. Therefore, this suggests that for those with a larger body mass index, then the ankle stiffness must also be greater. These combined effects would tend to improve postural stability.

Acknowledgements

This study was supported, in part, by funds from the Henry H. Kessler Foundation. Portions of the project were presented at the annual meetings of the Association of Academic Physiatrists, 2003, and the Gait and Clinical Movement Analysis Society, 2004.

Appendix A. Supplementary data

Supplementary data associated with this article can be found, in the online version, at [doi:10.1016/j.gaitpost.2006.05.009](https://doi.org/10.1016/j.gaitpost.2006.05.009).

References

- [1] Winter DA, Patla AE, Prince F, Ishac M, Gielo-Perczak K. Stiffness control of balance in quiet standing. *J Neurophysiol* 1998;80:1211–21.
- [2] Winter DA, Patla AE, Rietdyk S, Ishac MG. Ankle muscle stiffness in the control of balance during quiet standing. *J Neurophysiol* 2001;85:2630–3.
- [3] Kirsch RF, Kearney RE. Identification of time-varying stiffness dynamics of the human ankle joint during an imposed movement. *Exp Brain Res* 1997;114:71–85.
- [4] Mirbagheri MM, Barbeau H, Kearney RE. Intrinsic and reflex contributions to human ankle stiffness: variation with activation level and position. *Exp Brain Res* 2000;135:423–36.
- [5] Morasso PG, Sanguineti V. Ankle muscle stiffness alone cannot stabilize balance during quiet standing. *J Neurophysiol* 2002;88:2157–62.
- [6] Farley CT, Houdijk HH, Van Strien C, Louie M. Mechanism of leg stiffness adjustment for hopping on surfaces of different stiffnesses. *J Appl Physiol* 1998;85:1044–55.
- [7] Noth J, Matthew H, Friedemann H. Long latency reflex force of human finger muscles in response to imposed sinusoidal movements. *Exp Brain Res* 1984;55:317–24.
- [8] Morasso PG, Schieppati M. Can muscle stiffness alone stabilize upright standing? *J Neurophysiol* 1999;82:1622–6.
- [9] Hof AL. In vivo measurement of the series elasticity release curve of human triceps surae muscle. *J Biomech* 1998;31:793–800.
- [10] Soames RW, Atha J. The validity of physique-based inverted pendulum models of postural sway behavior. *Annu Hum Biol* 1980;7:145–53.
- [11] Suzuki M, Yamazaki Y, Matsunami K. Simplified dynamics model of planar two-joint arm movements. *J Biomech* 2000;33:925–31.

- [12] Blajer W, Czaplicki A. Modeling and inverse simulation of somersaults on the trampoline. *J Biomech* 2001;34:1619–29.
- [13] Nicholas SC, Doxey-Gasway DD, Paloski WH. A link-segment model of upright human posture for analysis of head-trunk coordination. *J Vestib Res* 1998;8:187–200.
- [14] Farley CT, Morgenroth DC. Leg stiffness primarily depends on ankle stiffness during human hopping. *J Biomech* 1999;32:267–73.
- [15] Iqbal K, Pai Y. Predicted region of stability for balance recovery: motion at the knee joint can improve termination of forward movement. *J Biomech* 2000;33:1619–27.
- [16] Edwards WT. Comments on Predicted region of stability for balance recovery: motion at the knee joint can improve termination of forward movement'. *J Biomech* 2001;34:831–2.
- [17] Chaffin DB, Andersson GJ. *Occupational biomechanics* New York: John Wiley & Sons; 1984.
- [18] Johansson R, Magnusson M, Akesson M. Identification of human postural dynamics. *IEEE Trans Biomed Eng* 1988;35:858–69.
- [19] Masani K, Popovic MR, Nakazawa K, Kouzaki M, Nozaki D. Importance of body sway velocity information in controlling ankle extensor activities during quiet stance. *J Neurophysiol* 2003;90:3774–82.
- [20] Peterka RJ. Sensorimotor integration in human postural control. *J Neurophysiol* 2002;88:1097–118.
- [21] Jeka J, Kiemel T, Creath R, Horak F, Peterka R. Controlling human upright posture: velocity information is more accurate than position or acceleration. *J Neurophysiol* 2004;92:2368–79.
- [22] Casadio M, Morasso PG, Sanguineti V. Direct measurement of ankle stiffness during quiet standing: implications for control modelling and clinical application. *Gait Posture* 2005;21:410–24.
- [23] Loram ID, Lakie M. Direct measurement of human ankle stiffness during quiet standing: the intrinsic mechanical stiffness is insufficient for stability. *J Physiol* 2002;545:1041–53.
- [24] Weiss PL, Hunter IW, Kearney RE. Human ankle joint stiffness over the full range of muscle activation levels. *J Biomech* 1988;21:539–44.
- [25] Lark SD, Buckley JG, Bennett S, Jones D, Sargeant AJ. Joint torques and dynamic joint stiffness in elderly and young men during stepping down. *Clin Biomech (Bristol Avon)* 2003;18:848–55.
- [26] McHugh MP, Hogan DE. Effect of knee flexion angle on active joint stiffness. *Acta Physiol Scand* 2004;180:249–54.
- [27] Horak FB, Nashner LM. Central programming of postural movements: adaptation to altered support-surface configurations. *J Neurophysiol* 1986;55:1369–81.
- [28] Kuo AD, Zajac FE. Human standing posture: multi-joint movement strategies based on biomechanical constraints. *Progr Brain Res* 1993;97:349–58.
- [29] Runge CF, Shupert CL, Horak FB, Zajac FE. Ankle and hip postural strategies defined by joint torques. *Gait Posture* 1999;10:161–70.
- [30] Aramaki Y, Nozaki D, Masani K, Sato T, Nakazawa K, Yano H. Reciprocal angular acceleration of the ankle and hip joints during quiet standing in humans. *Exp Brain Res* 2001;136:463–73.
- [31] Fitzpatrick R, Rogers DK, McCloskey DI. Stable human standing with lower-limb muscle afferents providing the only sensory input. *J Physiol* 1994;480(Pt 2):395–403.
- [32] Young Y, Myers AH, Provenzano G. Factors associated with time to first hip fracture. *J Aging Health* 2001;13:511–26.
- [33] Taggart H, Craig D, McCoy K. Healthy elderly individuals do not inevitably lose bone density and weight as they age. *Arch Gerontol Geriatr* 2004;39:283–90.